DES AND URANS DOWNSTREAM OF A HEATED BACKWARD-FACING STEP

S. Ruck, F. Arbeiter
First Thermal and Fluids Engineering Summer Conference, August 2015, New York

INSTITUTE OF NEUTRON PHYSICS AND REACTOR TECHNOLOGY

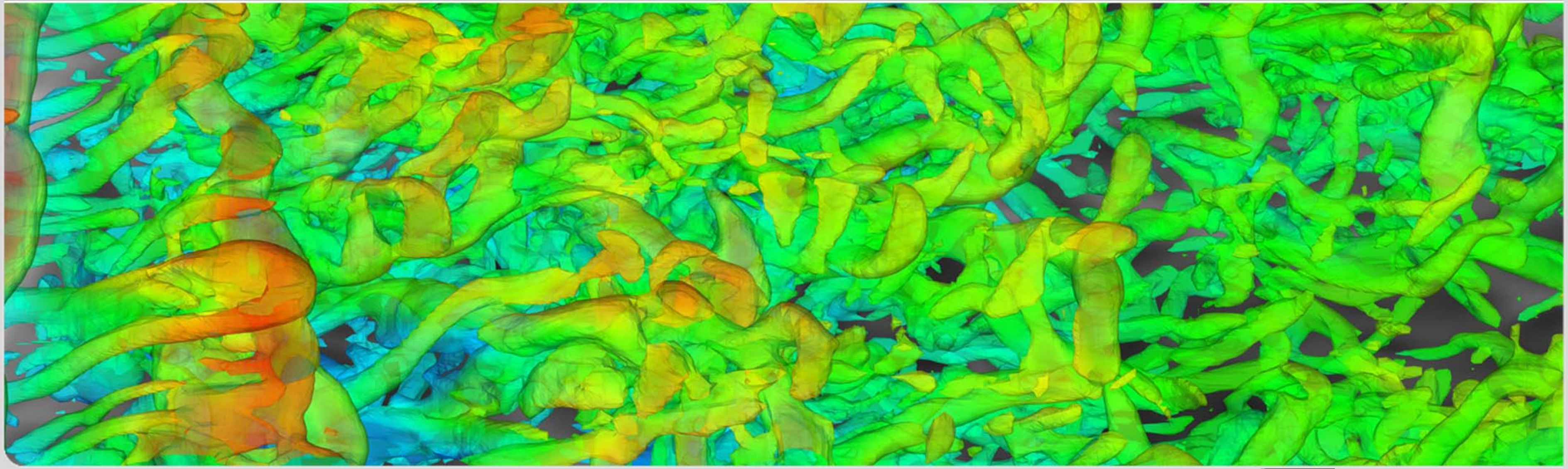

Introduction

Motivation

- Validated “tool” for an accurate thermohydraulic prediction of heated, turbulent flow to develop new designs of thermally high loaded cooling channels with <u>structured</u> or <u>rib-roughened</u> walls.
  - Cooling the plasma-faced 1st wall of fusion reactor (~700-1000°C, ~0.75 MW/m^2)

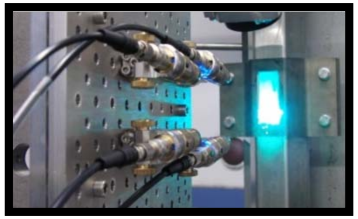

➡ Experimental Methods
- PIV, LDA measurements, Infrared Camera
- Thermocouple and pressure tabs

➡ **Computational Fluid Dynamics**
- Not limited to global performance estimations
- Capturing transient 3d-effects
- Thermal and fluid fields are resolved simultaneously

➡ CFD is very sensitive to the numerical method and turbulence treatment

Institute of Neutron Physics and Reactor Technology
Measurement Technology and Experimental Methods (MET)

Methods

Numerical Methods

- Reynolds-Averaged-Navier-Stokes (RANS) + isotropic EVM
  - Inaccurate flow and heat transfer prediction [Acharya 1993, Ooi 2002]
- Large Eddy Simulations (LES)
  - Accurate flow and heat transfer prediction [Labbé 2013,Tafti 2005]
  - Limited for engineering applications by its demanding grid requirements
- Hybrid RANS/LES
  - Detached Eddy Simulations (DES) for high-Reynolds number, massively separated flows [Spalart, 1997]
  - Only a few studies of internal turbulent flows with heat transfer
  - Accurate thermohydraulic predictions for heated, rib-roughened channel flow [Viswanathan 2005; 2006]) at moderate Re=2E4.

⇨ Validation of DES for boundary conditions of plasma-faced 1st wall of fusion reactors

Boundary Conditions

Plasma-Faced 1st Wall

- $10E3 < Re_{Dh} < 150E3$; $Re_{Dh,Operating} = 1{,}05E5$
- Asymmetrically heated cooling channels
- 15 x 15 mm with 2 mm round edges, rib-pitch-to-rib-height-ratio of p/e=10, rib-height-to-hyd.-diameter-ratio of e/Dh=0.0638
- High pressure 8-MPa-helium gas
  - No experimental data at the operating conditions
    - ⇨ Experiments were designed, installed and will be carried out soon

- 1st Step - Validation with **Heated Backward Facing Step Flow**
  - Numerous experimental [Vogel 1984; Adams 1984] and numerical [Keating 2001] benchmark data for $Re_h=2.8E4$ are present
  - Scaling flow conditions from benchmark to a 4h x 4h channel, step height h = 3.8 mm, 8-MPa-helium gas, $Re_h=2.8E4 \Rightarrow Re_{Dh}=1.12E5$

Methods

Simulation Overview

- Computational Domain
  - 27 h x 4 h x 4 h: 181 x 78 x 108, expansion ratio of 1.25
  - Local grid refinement behind the step to generate a focus region
  - 2.8 Mio Cells
- Boundary Conditions
  - Constant heat flux density at the lower bottom wall
  - Fluid with ideal gas conditions
- Inflow Conditions
  - Periodic flow simulations
  - Re_h=2.8E4 ⇨ Re_{Dh}=1.12E5

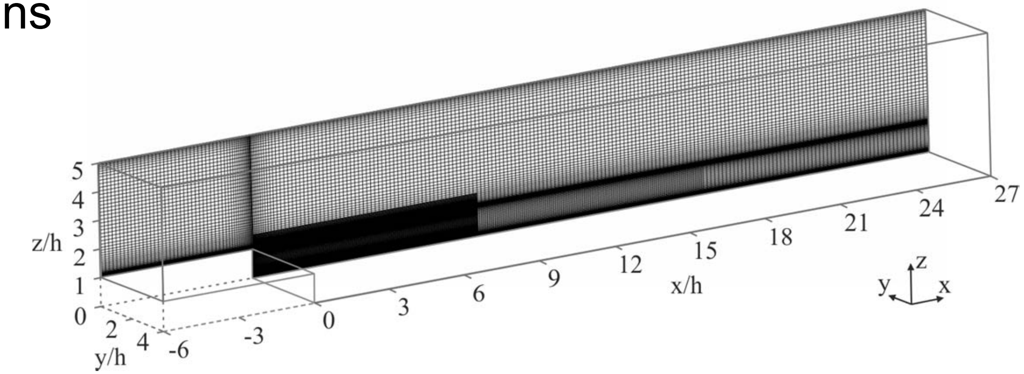

Methods

Simulation Overview

- Numerical approach
  - Delayed DES and URANS
    - k-ε-realizable-model and k-ω-SST-model
  - Segregated Solver / Fluent V.15
    - Convective terms: QUICK & UW Scheme
      - Momentum Equation: DES BCD; URANS: QUICK
    - Diffusion terms: 2nd CD Scheme
    - Pressure: 2nd Scheme
    - Temporal: Bounded 2nd Imp. Scheme
- Simulation time
  - After received a fully developed flow field, the simulation were run 10 flow-throughs for DES and 3 flow-throughs for URANS
- Results
  - Spatial average: 10 spanwise positions
  - Temporal average: 10 flow-throughs for DES, 3 flow-throughs for URANS

Flow Field

DES

- Free shear layer are formed by flow separation at the edge of the step
- Reattachment XR≈6h
  - Spanwise limitation of computational domain
- Recirculation and redeveloping regions
- Flow structures caused by the flow separation either impact on the bottom wall or flow further downstream
  - Impingement ones move upstream or downstream
  - Cooling Effect
    - Transporting colder fluid from the core flow toward the heated wall
    - Reducing the viscous sublayer and heat transfer is enhanced
    - Maximum occur in the vicinity of reattachment

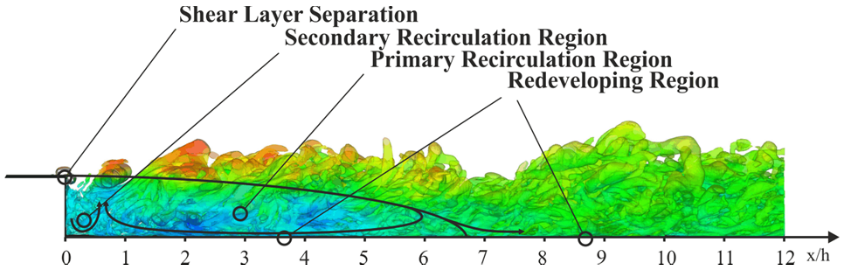

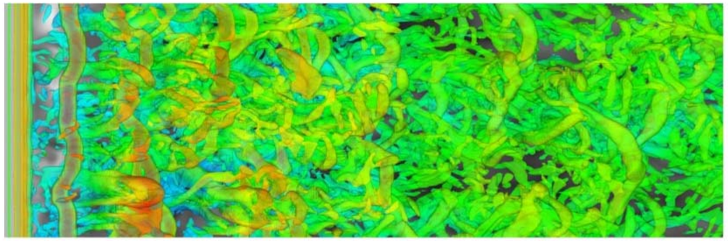

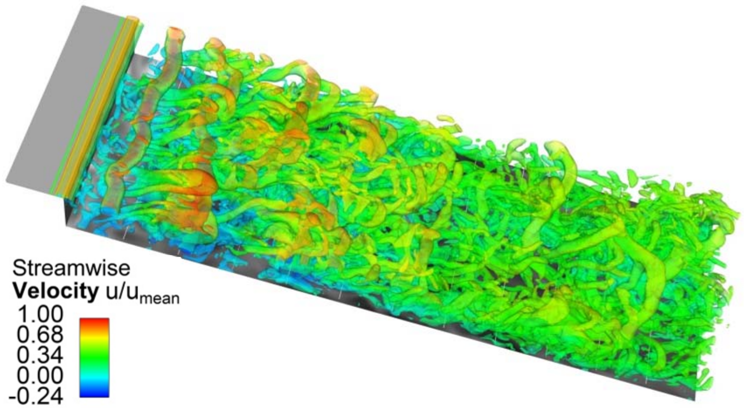

Flow Field

DES

- Free shear layer are formed by flow separation at the edge of the step
- Reattachment XR≈6h
  - Spanwise limitation of computational domain
- Recirculation and redeveloping regions
- Flow structures caused by the flow separation either impact on the bottom wall or flow further downstream
  - Impingement ones move upstream or downstream
  - Cooling Effect
    - Transporting colder fluid from the core flow toward the heated wall
    - Reducing the viscous sublayer and heat transfer is enhanced
    - Maximum occurs in the vicinity of reattachment

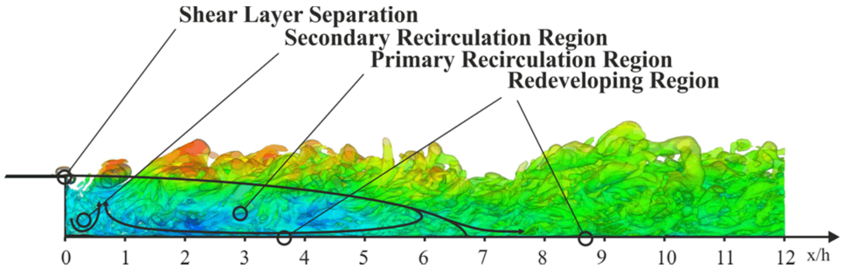

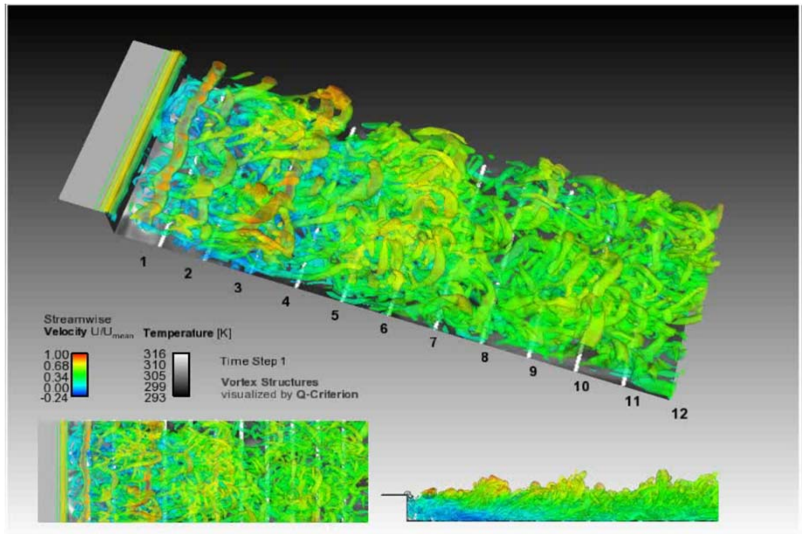

Flow Field

DES

- Free shear layer are formed by flow separation at the edge of the step
- Reattachment XR≈6h
  - Spanwise limitation of computational domain
- Recirculation and redeveloping regions
- Flow structures caused by the flow separation either impact on the bottom wall or flow further downstream
  - Impingement ones move upstream or downstream
  - Cooling Effect
    - Transporting colder fluid from the core flow toward the heated wall
    - Reducing the viscous sublayer and heat transfer is enhanced
    - Maximum occurs in the vicinity of reattachment

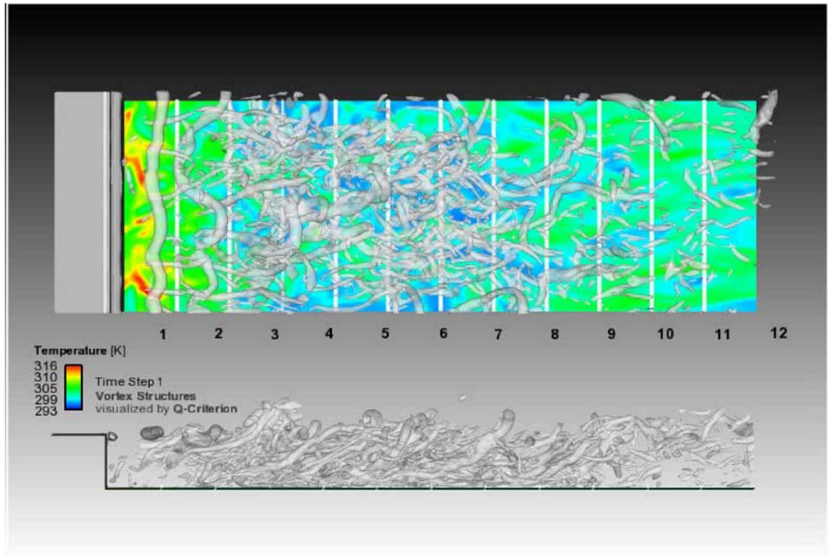

Local Heat Transfer

DES

- Acceptable agreement with experiments
- Difference upstream of reattachment
  - Insufficient spatial average
- Drifting downstream of reattachment
  - Correlates with the end of the focus region

URANS

- Close to the step, URANS results differ from experiments
- Except the minimum and maximum values, k-ω-SST agrees well
- k-ε-reali. differs enormously
  - 60% for peaks

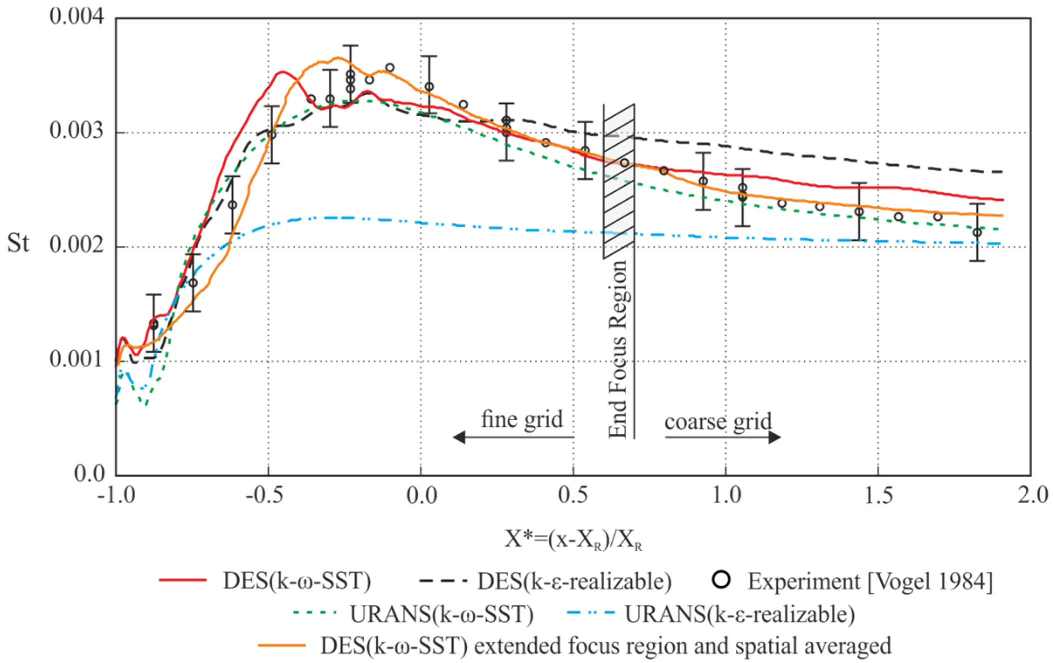

Temperature Distributions

DES & URANS

- Temperature gradients at the near wall region are similar for DES and URANS and start to differ with increasing wall distance
  - Influence of turbulence heat transfer increase
- Except very close to the step, DES results are in good agreement with experiments and URANS results differ
  - High gradients across the free shear layer for URANS
    - Underprediction of turbulent mixing
    - Correlates with an underprediction of turbulent flux
    - Yield higher surface temperatures

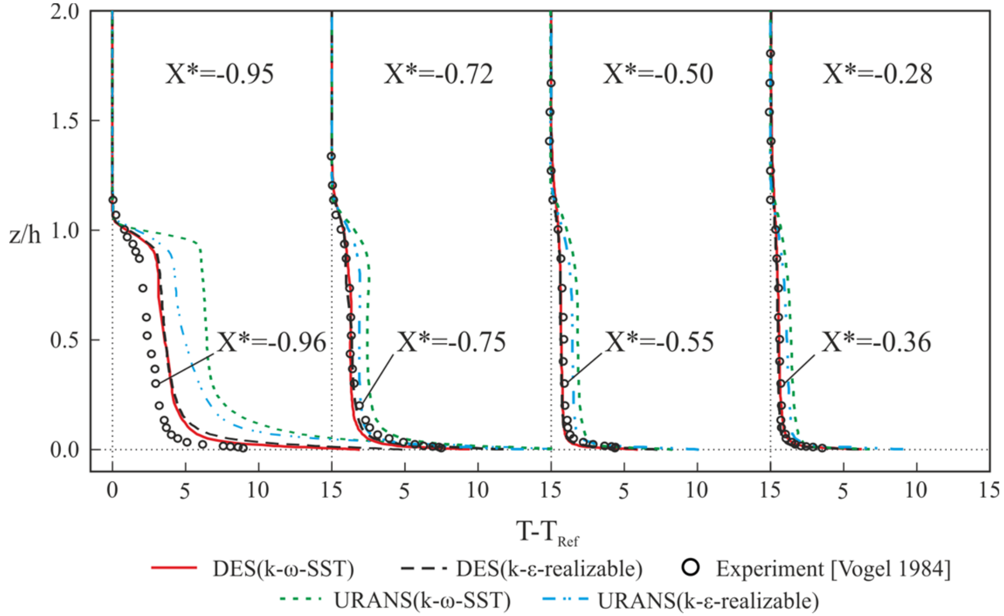

Turbulent Heat Flux

DES

- DES show similar trends to LES results
- Peaks in the free shear layer and wall boundary layer
- High turbulent mixing
  - Associated with turbulent large-scale eddies
  - Gradients decrease further downstream and vanish with flow reattachment
- Downstream of reattachment heat transfer occurs mostly at the bottom wall

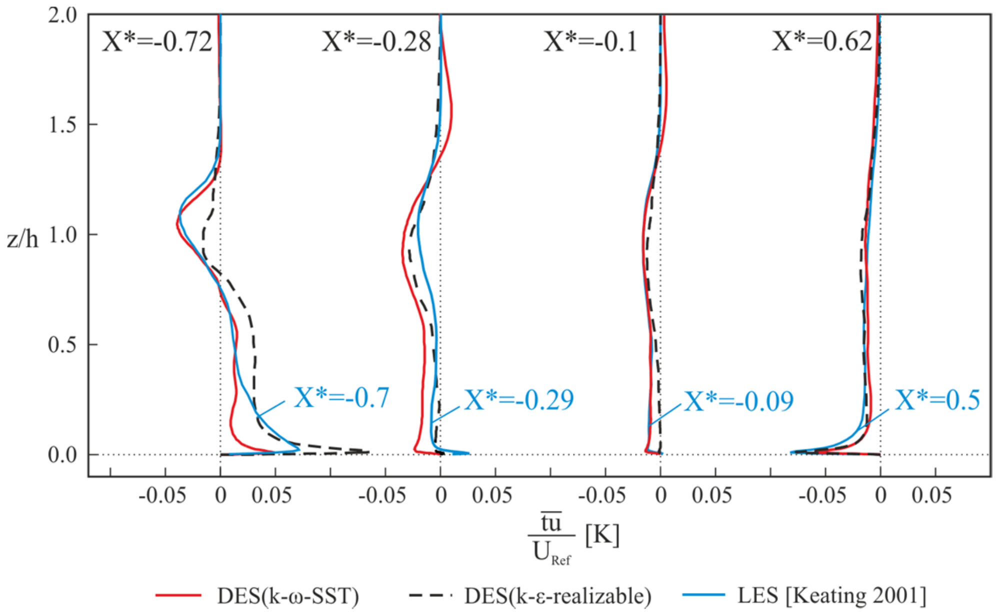

Turbulent Fluctuations

u_{RMS} , v_{RMS} and w_{RMS}

- DES results show good agree with experiments
  - Distribution are well predicted (by the DES(k-ω-SST))
  - Peak values are overpredicted (by the DES(k-ε-reali.))
  - Maximum is reached upstream of reattachment
  - $U_{RMS} > W_{RMS}, V_{RMS}$

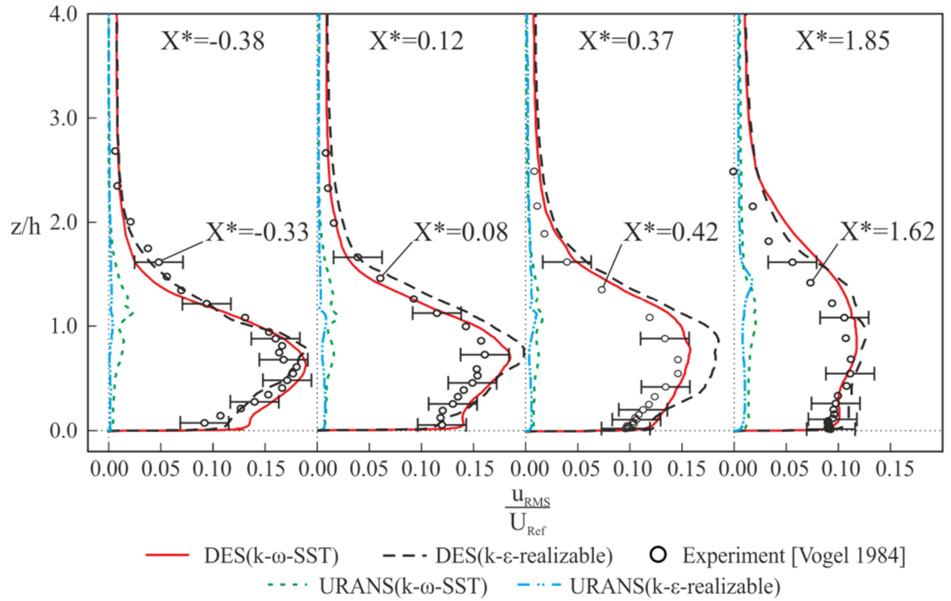

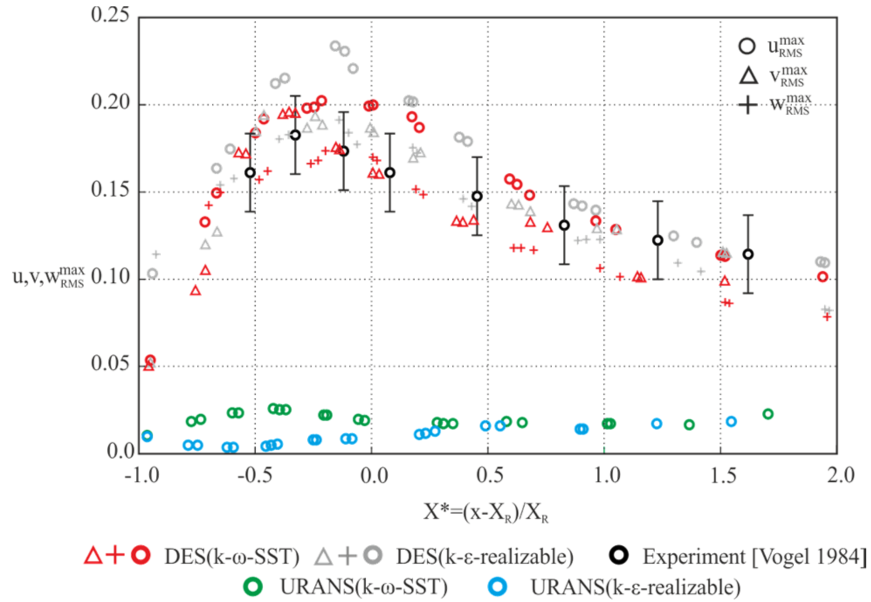

Summary

Overview

- Transient flow field was well reproduced by DES
- Temperature levels and heat transfer at the bottom wall were accurately determined by DES
- Significant turbulent heat transfer occurs across the shear layer and is triggered by turbulent large-scale flow structures. It is well resolved by DES.

➡ Results of the 1st Step - Validation with Heated Backward Facing Step Flow: **DES is promising approach for thermohydraulic prediction of turbulent flows**. Ongoing research focus on an extended validation for high Reynolds number flow in heated, rib-roughened channels at boundary conditions of plasma-faced 1st wall of fusion reactors

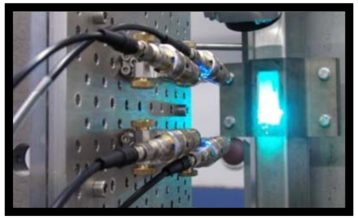

DES AND URANS DOWNSTREAM OF A HEATED BACKWARD-FACING STEP

S. Ruck, F. Arbeiter

First Thermal and Fluids Engineering Summer Conference, August 2015, New York

INSTITUTE OF NEUTRON PHYSICS AND REACTOR TECHNOLOGY

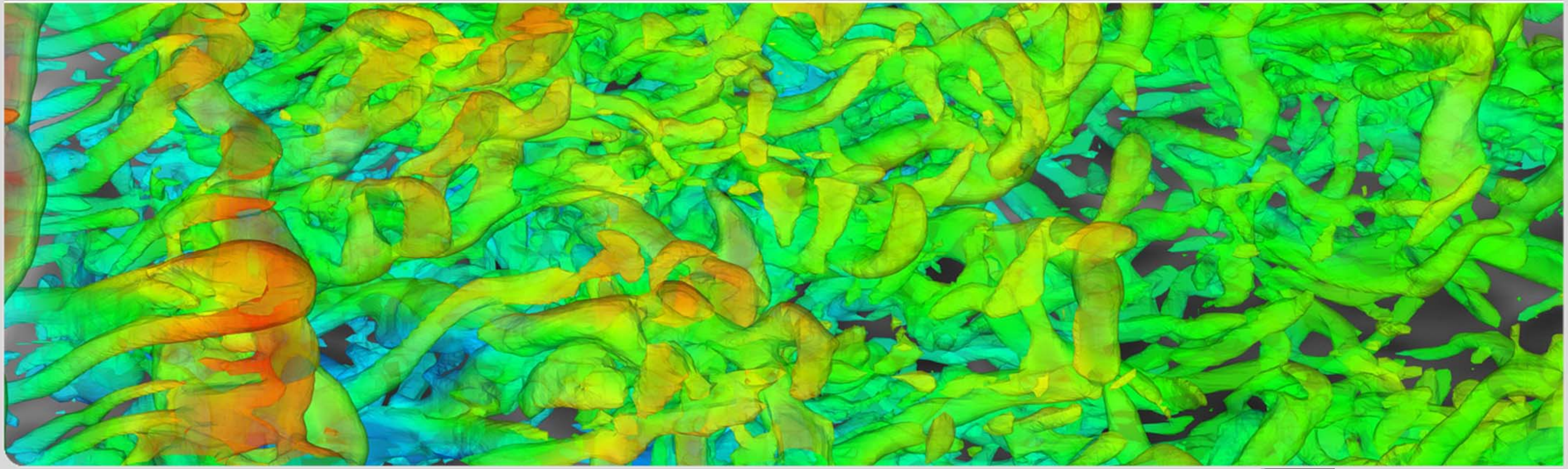

Appendix

Detached Eddy Simulation

- It is a non-zonal approach providing a single smooth velocity field.
- Uniform turbulence model taking the (integral) turbulence length scale and the spatial grid density into account
  - regions where the maximum spatial grid density is much smaller than the flow turbulence length scale: LES mode
  - regions where the maximum spatial grid density is greater than the flow turbulence length scale: RANS mode
- Subdivision of the computational domain into regions of LES (separated flow regions) and RANS (boundary layers, near wall region) quality.

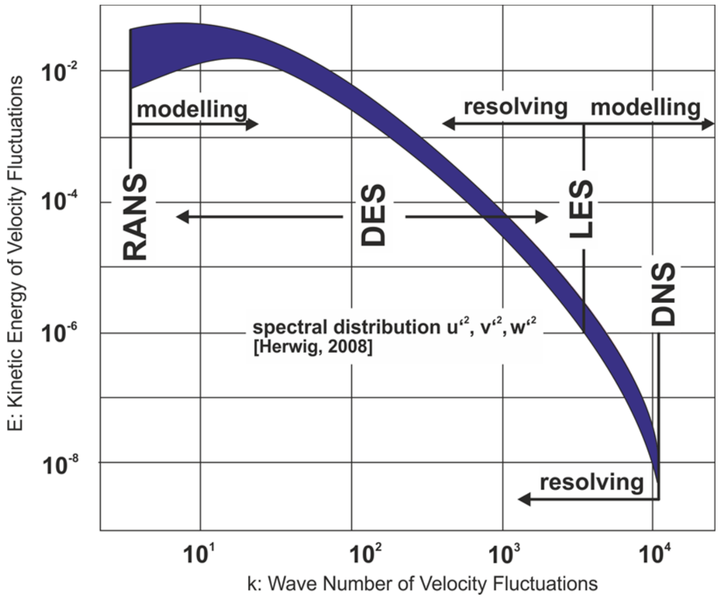

Methods

Detached Eddy Simulation

- Uniform turbulence model concept taking the (integral) turbulence length scale and the spatial grid density into account
  - regions where $\Delta_{\max} < C \cdot l_t$: DES functions in LES mode
  - regions where $\Delta_{\max} > C \cdot l_t$: DES functions in RANS mode
- Introducing a gird dependent length-scale into the destruction term
  - 2E-EVM: Destruction term of the k-equation [Strelets, 2001]

$$\widetilde{D}_k = \overline{\rho} \cdot \frac{k^{3/2}}{l_t^k} \rightarrow D_{DES} = \overline{\rho} \cdot \frac{k^{3/2}}{l_t^{DES}} \qquad l_t^{DES} = \min\left[l_t^k, C_{DES}^k \cdot \Delta_{max}\right]$$

    - k-ε-realizable-model $l_t^k = \frac{k^{3/2}}{\varepsilon}$; k-ω-SST-model $l_t^k = \frac{k^{1/2}}{\beta^* \cdot \omega}$
  - RANS Mode $\nu_t = C_\mu \cdot \frac{k^2}{\varepsilon}$; $\nu_t = \frac{k}{\omega} \cdot \frac{1}{\max\left[\frac{1}{\alpha^*}, \frac{S \cdot F_2}{a_1 \cdot \omega}\right]}$
  - LES Mode $\nu_{SGS} = C_k \cdot k_{SGS}^{1/2} \cdot \overline{\Delta}$

$$l_t^{DDES} = l_t^k - f_{DDES} \cdot \max\left[0, l_t^k - C_{DES}^k \cdot \Delta_{max}\right]$$

Appendix

Detached Eddy Simulation

- Favre-averaging (RANS) or -filtering (LES) the governing flow equations and decomposing flow quantities into resolved and unresolved ones introduces turbulence closure terms [Garnier, 2009][Hirsch, 1988].
  - Momentum equation: Reynolds stresses τ_{ij}^{t} or subgrid-scale stresses τ_{ij}^{SGS}
  - Energy equation: Reynolds heat flux Q_{ij}^{SGS} and subgrid-scale heat flux Q_{ij}^{t}
- Boussinesq hypothesis: deviatoric portion of the stresses are related by the eddy-viscosity to the mean and resolved strain-rate tensor respectively (RANS: ν_t, LES: ν_{SGS})
- Heat fluxes are approximated by correlating the energy flux of the unresolved and modelled scales with the gradients of the resolved or mean temperatures and a turbulent thermal conductivity (RANS: $\kappa_t \sim \nu_t \cdot Pr_t^{-1}$, LES: $\kappa_{SGS} \sim \nu_{SGS} \cdot {Pr_{SGS}}^{-1}$)

Institute of Neutron Physics and Reactor Technology
Measurement Technology and Experimental Methods (MET)

Appendix

Detached Eddy Simulation

- Favre-averaged flow equations
  - Momentum equation

$$\frac{\partial}{\partial t}(\overline{\rho}\cdot\tilde{u}_i)+\frac{\partial}{\partial x_j}(\overline{\rho}\cdot\tilde{u}_i\cdot\tilde{u}_j)=\overline{f}_i-\frac{\partial\overline{p}}{\partial x_i}+\frac{\partial}{\partial x_j}\tilde{\tau}_{ij}^{mol}+\frac{\partial}{\partial x_j}\tau_{ij}^{t}$$

$$\tau_{ij}^{t}=-\overline{\rho\cdot u''_i\cdot u''_j}\quad\rightarrow\quad\tau_{ij}^{t}=2\cdot\overline{\rho}\cdot\nu_t\cdot\left(\tilde{S}_{ij}-\frac{1}{3}\cdot\tilde{S}_{kk}\cdot\delta_{ij}\right)-\frac{2}{3}\cdot\overline{\rho}\cdot\tilde{k}\cdot\delta_{ij}$$

  - Energy euquation

$$\frac{\partial}{\partial t}(\overline{\rho}\cdot\tilde{h})+\frac{\partial}{\partial x_j}(\overline{\rho}\cdot\tilde{u}_j\cdot\tilde{h})+\frac{\partial\tilde{q}_j}{\partial x_j}-\frac{\partial\overline{p}}{\partial t}-\tilde{u}_j\cdot\frac{\partial\overline{p}}{\partial x_j}-\tilde{\Phi}=-\frac{\partial}{\partial x_j}Q_j^t+\overline{u_j''\cdot\frac{\partial p}{\partial x_j}}$$

$$Q_j^t=-\overline{\rho\cdot u''_i\cdot h''}\quad\rightarrow\quad Q_j^t=-\frac{\overline{\rho}\cdot\nu_t\cdot C_p}{Pr_t}\cdot\frac{\partial\tilde{T}}{\partial x_j}$$

Appendix

Detached Eddy Simulation

- Favre-filtered flow equations
  - Momentum equation

$$\frac{\partial}{\partial t}(\overline{\rho}\cdot\tilde{u}_i)+\frac{\partial}{\partial x_j}(\overline{\rho}\cdot\tilde{u}_i\cdot\tilde{u}_j)=\overline{f}_i-\frac{\partial\overline{p}}{\partial x_i}+\frac{\partial}{\partial x_j}\tilde{\tau}_{ij}^{mol}-\frac{\partial}{\partial x_j}\tau_{ij}^{SGS}$$

$$\tau_{ij}^{SGS}=\overline{\rho}\cdot\left(\widetilde{u_i\cdot u_j}-\tilde{u}_i\cdot\tilde{u}_j\right)\quad\rightarrow\quad\tau_{ij}^{SGS}=-2\cdot\overline{\rho}\cdot\nu_{SGS}\cdot\left(\tilde{S}_{ij}-\frac{1}{3}\cdot\tilde{S}_{kk}\cdot\delta_{ij}\right)+\frac{1}{3}\cdot\tau_{kk}^{SGS}\cdot\delta_{ij}$$

  - Energy equation

$$\frac{\partial}{\partial t}(\overline{\rho}\cdot\tilde{h})+\frac{\partial}{\partial x_j}(\overline{\rho}\cdot\tilde{u}_j\cdot\tilde{h})+\frac{\partial\tilde{q}_j}{\partial x_j}-\frac{\partial\overline{p}}{\partial t}-\tilde{u}_j\cdot\frac{\partial\overline{p}}{\partial x_j}-\tilde{\Phi}=-C_p\cdot\frac{\partial}{\partial x_j}Q_j^{SGS}$$

$$Q_j^{SGS}=\overline{\rho}\cdot\left(\widetilde{T\cdot u_j}-\tilde{T}\cdot\tilde{u}_j\right)\quad\rightarrow\quad Q_j^{SGS}=-\frac{\overline{\rho}\cdot\nu_{SGS}}{Pr_{SGS}}\cdot\frac{\partial\tilde{T}}{\partial x_j}$$

Appendix

Detached Eddy Simulation

- Favre-filtered flow equations
  - Momentum equation

$$\frac{\partial}{\partial t}(\overline{\rho}\cdot\tilde{u}_i)+\frac{\partial}{\partial x_j}(\overline{\rho}\cdot\tilde{u}_i\cdot\tilde{u}_j)=\overline{f}_i-\frac{\partial\overline{p}}{\partial x_i}+\frac{\partial}{\partial x_j}\tilde{\tau}_{ij}^{mol}-\frac{\partial}{\partial x_j}\tau_{ij}^{SGS}$$

$$\tau_{ij}^{SGS}=\overline{\rho}\cdot\left(\widetilde{u_i\cdot u_j}-\tilde{u}_i\cdot\tilde{u}_j\right)\ \rightarrow\ \tau_{ij}^{SGS}=-2\cdot\overline{\rho}\cdot\nu_{SGS}\cdot\left(\tilde{S}_{ij}-\frac{1}{3}\cdot\tilde{S}_{kk}\cdot\delta_{ij}\right)+\frac{1}{3}\cdot\tau_{kk}^{SGS}\cdot\delta_{ij}$$

  - Energy equation

$$\frac{\partial}{\partial t}(\overline{\rho}\cdot\tilde{h})+\frac{\partial}{\partial x_j}(\overline{\rho}\cdot\tilde{u}_j\cdot\tilde{h})+\frac{\partial\tilde{q}_j}{\partial x_j}-\frac{\partial\overline{p}}{\partial t}-\tilde{u}_j\cdot\frac{\partial\overline{p}}{\partial x_j}-\tilde{\Phi}=-C_p\cdot\frac{\partial}{\partial x_j}Q_j^{SGS}$$

$$Q_j^{SGS}=\overline{\rho}\cdot\left(\widetilde{T\cdot u_j}-\tilde{T}\cdot\tilde{u}_j\right)\ \rightarrow\ Q_j^{SGS}=-\frac{\overline{\rho}\cdot\nu_{SGS}}{Pr_{SGS}}\cdot\frac{\partial\tilde{T}}{\partial x_j}$$

Appendix

Detached Eddy Simulation

- k-equation

$$\frac{\partial}{\partial t}(\overline{\rho}\cdot k)+\frac{\partial}{\partial x_i}(\overline{\rho}\cdot k\cdot\tilde{u}_i)=\frac{\partial}{\partial x_j}\left[(\overline{\mu}+\sigma_k\cdot\overline{\rho}\cdot\nu_t)\cdot\frac{\partial k}{\partial x_j}\right]+\tilde{P}_k+D_k+S_k$$

- Destruction term

$$D_k=\overline{\rho}\cdot\frac{k^{3/2}}{l_t}\rightarrow D_{DES}=\overline{\rho}\cdot\frac{k^{3/2}}{l_t^{DES}}\qquad l_t^{DES}=\min\left[l_t^k, l_t^{LES}\right]\qquad l_t^{LES}=C_{DES}^k\cdot\Delta_{max}$$

  - k-ε-realizable-model [Ansys]

$$l_t^k=\frac{k^{3/2}}{\varepsilon}\qquad C_{DES}^k=0.61$$

  - k-ω-SST-model [Strelets, 2001] [Menter, 1994]

$$l_t^k=\frac{k^{1/2}}{\beta^*\cdot\omega}\qquad C_{DES}^k=(1-F_1)\cdot C_{DES}^{k-\varepsilon}+F_1\cdot C_{DES}^{k-\omega};\ C_{DES}^{k-\varepsilon}=0.61;\ C_{DES}^{k-\omega}=0.78$$

Appendix

Motivation

- RANS mode
  - Two-equation k-ω-SST model, k-ε-realizable-model

$$\nu_t = \frac{k}{\omega} \cdot \frac{1}{\max\left[\frac{1}{\alpha^*}, \frac{S \cdot F_2}{a_1 \cdot \omega}\right]} ; \nu_t = C_\mu \cdot \frac{k^2}{\varepsilon};$$

- LES mode
  - Turbulent kinetic energy is considered as subgrid-scale kinetic energy $k \rightarrow k_{SGS}$
  - Dynamic Kinetic Energy Subgrid-Scale Model [Kim, Menon, 1997] [Kim, 2004]

$$\nu_{SGS} = C_k \cdot k_{SGS}^{1/2} \cdot \overline{\Delta}$$

$$\tau_{ij}^{SGS} = -2 \cdot \overline{\rho} \cdot C_k \cdot k_{SGS}^{1/2} \cdot \overline{\Delta} \cdot \tilde{S}_{ij} + \frac{2}{3} \cdot \overline{\rho} \cdot k_{SGS} \cdot \delta_{ij}$$

$$\overline{\Delta} = V[\Delta x, \Delta y, \Delta z]^{1/3}$$